Characterization of toxic effects of NH_4^+ on growth and its alleviation by NO_3^-. J. Amer. Soc. Hort. Sci. 107:125–129.
10. Gruttadaurio, J. (ed.). 1982. Cornell poinsettia guidelines for 1982. Dept. of Floriculture and Ornamental Horticulture, Cornell Univ., Ithaca, N.Y. (Mimeo).
11. Hoagland, D.R. and D.I. Arnon. 1950. The water-culture method of growing plants without soil. Ca. Agr. Expt. Sta. Cir. 347. (Rev. ed.).
12. MacLeod, L.B. and R.B. Carson. 1966. Influence of K on yield and chemical composition of grasses grown in hydroponic culture with 12, 50 and 75% of the N supplied as NH_4^+. Agron. J. 58:52–57.
13. Maynard, D.N. and A.V. Barker. 1969. Studies on the tolerance of plants to ammonium nutrition. J. Amer. Soc. Hort. Sci. 94:235–239.
14. McElhannon, W.S. and H.A. Mills. 1978. Influence of percent NO_3^-/NH_4^+ on growth, N absorption and assimilation by lima beans in solution culture. Agron. J. 70:1027–1032.
15. Munn, D.A. and W.A. Jackson. 1978. Nitrate and ammonium uptake by rooted cuttings of sweet potato. Agron. J. 70:312–316.
16. Patnaik, R., A.V. Barker, and D.N. Maynard. 1972. Effects of ammonium and potassium ions on some physiological and biochemical processes of excised cucumber cotyledons. Physiol. Plant. 27:32–36.
17. Pierpont, R.A. and P.L. Minotti. 1977. Effects of calcium carbonate on ammonium assimilation by tomato seedlings. J. Amer. Soc. Hort. Sci. 102:20–23.
18. Purtich, G.S. and A.V. Barker. 1967. Structure and function of tomato leaf chloroplasts during ammonium toxicity. Plant Physiol. 42:1229–1238.
19. Sasseville, D.N. and H.A. Mills. 1979. N form and concentration: Effects on N absorption, growth, and total N accumulation with southernpeas. J. Amer. Soc. Hort. Sci. 104:586–591.
20. Shanks, J.B. 1981. Poinsettias and their greenhouse culture. The Maryland Flor. 231.
21. Sheat, D.E.G., B.H. Fletcher, and H.E. Street. 1959. Studies on the growth of excised roots. VIII. The growth of excised tomato roots supplied with various inorganic sources of nitrogen. New Phytol. 58:128–141.
22. Steward, F.C. and H.E. Street. 1946. The soluble nitrogen fractions of potato tubers; the amides. Plant Physiol. 21:155–193.
23. Wakiuchi, N., H. Matsumoto, and E. Takahashi. 1971. Changes of some enzyme activities of cucumber during ammonium toxicity. Physiol. Plant. 24:248–253.
24. Wander, I.W. and J.W. Sites. 1956. The effects of ammonium and nitrate nitrogen with and without pH control on the growth of rough lemon seedlings. Proc. Amer. Soc. Hort. Sci. 68:211–226.
25. Wilcox, G.E., C.A. Mitchell, and J.E. Hoff. 1977. Influence of nitrogen form on exudation rate, and ammonium, amide, and cation composition of xylem exudate in tomato. J. Amer. Soc. Hort. Sci. 102:192–196.

J. Amer. Soc. Hort. Sci. 109(1):62–66. 1984.

An Optical Method for Estimating Papaya Maturity

G.S. Birth, G.G. Dull, J.B. Magee, H.T. Chan,[1] and C.G. Cavaletto[2]

Russell Research Center, Agricultural Research Service, U.S. Department of Agriculture, Athens, GA 30613

Additional index words. *Carica papaya*, nondestructive testing, transmittance spectroscopy

Abstract. **Body transmittance spectroscopy and analytical measurements of chlorophyll, carotenoids, and soluble solids concentrations were used to develop a nondestructive technique for estimating the maturity of papayas (*Carica papaya* L.). Optical measurements were taken between 500–900 nm with a scanning monochromator and a tilting-filter, abridged monochromator. Immature and mature-green fruit which were indistinguishable by visual examination could be separated by body transmittance spectroscopy into nonripening and ripening groups.**

A rapid, nondestructive means of identifying several stages of fruit development would be advantageous in order to provide consumers with high-quality papaya fruit. As the papaya develops from flower to ripe fruit, a number of physical and chemical changes occur (1, 6, 7): a) size increases; b) total sugars (on a fresh weight basis) increase from 3% to 9% (110 days after anthesis); c) seed color changes from white to black (110 days after anthesis); d) internal fruit flesh around periphery of seed cavity changes from white to yellow (120 days after anthesis); and e) the surface color changes from green to yellow (130 days after anthesis). These changes can be used to delineate specific stages of development.

Our primary objective was to develop a nondestructive means of distinguishing between immature and mature-green fruit. An immature fruit is one in which the seed and the flesh around the seed cavity is white. Seed in a mature-green fruit are turning black and the internal flesh has started to yellow. The external appearance of both the immature and mature-green fruit is green and indistinguishable by visual examination. A nondestructive technique which separates immature from mature-green fruit would have the following benefits: a) fruit might be harvested earlier, providing more shipping time and/or a longer shelf-life; b) the packer would be able to ship mature-green fruit which are presently discarded because ripeness cannot be predicted; and c) preliminary evidence suggests that fruit flies do not infest mature-green papayas (12). Shipment of mature-green fruit, therefore, may become the basis for an improved quarantine system for papaya. An instrumental method for distinguishing between immature and mature-green fruit in this laboratory would provide the basis for designing an instrument capable of making this separation in the field.

Received for publication 9 July 1982. Use of company or product name does not constitute an endorsement by USDA nor imply approval to the exclusion of other suitable products. The cost of publishing this paper was defrayed in part by the payment of page charges. Under postal regulations, this paper therefore must be hereby marked *advertisement* solely to indicate this fact.

[1]USDA-ARS, P.O. Box 917, Hilo, HI 96720.
[2]Dept. of Horticulture, University of Hawaii, Honolulu, HI 96822.

Materials and Methods

'Kapoho Solo' papaya fruit were obtained from a commercial source in the Kapoho area of the island of Hawaii, separated

into 5 maturity categories of immature, mature-green, quarter-ripe, half-ripe, and fully ripe, and shipped by air on the day of harvest to Athens, Ga., for analysis. The maturity categories were based on the procedure of Chen (7).

A biological spectrophotometer (5) was used to record the spectral data, the instrument being designed to provide a convenient means for changing the sample-detector geometry. The monochromator was computer-controlled and set to scan the wavelength region from 500–900 nm. Data were recorded in digital form at 300 discrete wavelengths. The radiant power available at the detector can be several orders of magnitude less than that incident on the fruit for some geometrical arrangements used in this work, so a detector with high detectivity was required. A 9558 EMI photomultiplier tube (PMT) was used to meet this requirement.

We utilized fiber optics to convey radiation from the fruit to a remote detector. In the sample-detector geometry used to obtain reflectance spectra (Fig. 1), the surface of the fruit was illuminated in the center of an area bounded by 4 evenly spaced fiber optics bundles. This provided a symmetrical collection of radiation from the fruit. For a body transmittance spectrum, the fruit was raised until it touched the short lengths of black latex tubing protecting the bundle tips (Fig. 2). The black tubing formed a seal against the fruit surface, prevented surface-reflected light from entering the fiber optics bundles, and protected the fruit from injury. Both sample-detector geometries (Fig. 1 and 2) are compatible with the biological spectrophotometer. The only difference between the 2 geometries is the position of the fruit.

An equation to predict nondestructively the pigment concentration and other attributes of papaya maturity was developed by first processing the data into a normalized derivative [i.e., the first derivative of transmittance with respect to wavelength divided by the transmittance, dT/T (3)] and then, after entering the chemical data into the computer, initiating a step-wise, multiregression analysis to obtain the appropriate regression equations. Regression equations were obtained for each wavelength and the computer program selected and printed out the equation that gave the lowest standard error (SE). The process could be repeated to add additional terms to the equation, thereby decreasing the SE further. The resulting equation is in the form:

$$C_1 = K_0 + K_1 X_{\lambda 1} + K_2 X_{\lambda 2} \qquad \text{[Eq. 1]}$$

where: C_1 is the predicted concentration of the first constituent; K_0, K_1, K_2 are the regression constants; X_λ = (dT/T) computed at wavelength λ.

An abridged, portable spectrophotometer was constructed using a tilting-filter system for wavelength scanning (11). The device consisted of 3 narrow bandpass interference filters mounted so that they could be rotated rapidly and sequentially through a collimated light beam. A change in the angle of incidence of the radiaiton on the filter occurred as it was rotated through the beam, which provided a change in the wavelength of the output radiation: this wavelength change constituted the scanning of a short spectral region, typically 8% of the filter's nominal wavelength. The data acquisition system recorded 100 data points for each filter. As a filter tilts, there are other changes in the nature of the spectra in addition to the change in wavelength. For

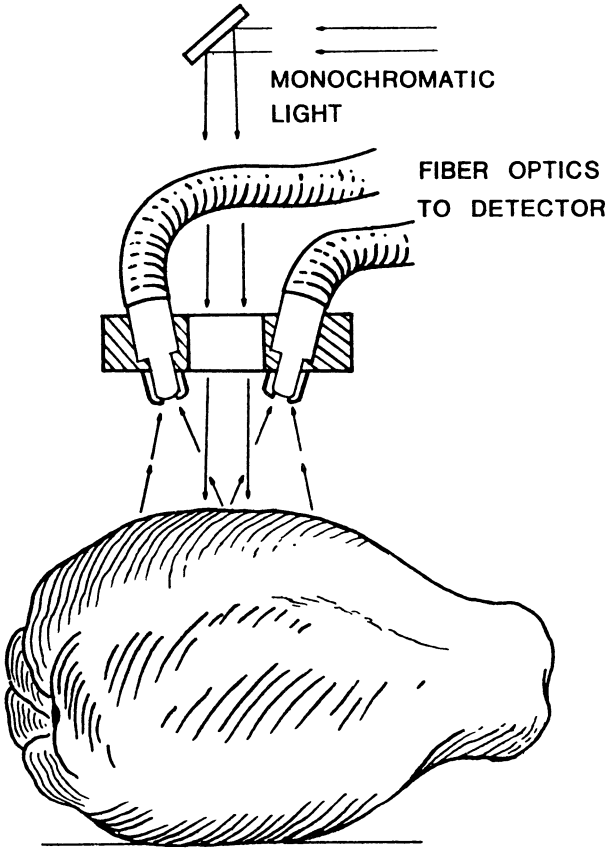

Fig. 1. Diagram of the geometry used to make body reflectance measurements on papaya. Only one pair of the fiber optics terminations (light take-off points) is shown in the cross-section sketch of the fiber optics holder.

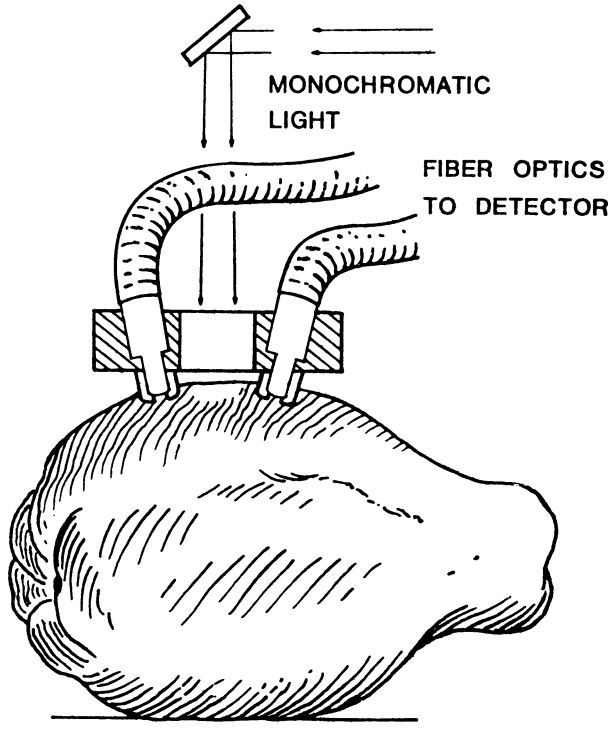

Fig. 2. Diagram of the geometry used to make body transmittance measurements on papaya. The apparatus for this measurement is identical to that shown in Fig. 1. Only the position of the fruit differs.

example, the bandpass increases and the relationship between changes in the angle of the tilting filter and the resulting wavelengths is not linear. For these reasons, the wavelengths that give the most accurate predictions with the tilting filter may differ from the wavelengths defined by the equation developed with the biological spectrophotometer. Consequently, the procedure used to implement the tilting-filter apparatus was to acquire filters that cover the appropriate wavelength range and independently calibrate the instrument with a regression analysis as described in the previous paragraph.

After recording spectral data for each fruit, 2 core samples (2.5-cm I.D. cork borer) were taken for chemical analyses within the area subtended by the rubber tubing on the fiber optics bundles. Part of each sample core nearest the seed cavity was removed to leave about 10 g of tissue, including peel, for analysis. Soluble solids content was estimated by refractometer measurements on juice squeezed from the core trimmings. Total chlorophyll content of one core sample was estimated as described by Harborne (8). To estimate total carotenoid pigments, the 2nd core sample was blended for 3 minutes in 50 ml of 60 hexane : 40 acetone (v/v) extracting solution. The blended sample was filtered and the absorbance of the filtrate was measured at 440 nm in a double-beam spectrophotometer against an extraction solution blank.

Results and Discussion

The carotenoid, chlorophyll, and soluble solids analyses of papaya at 5 different stages of maturity are given in Table 1. The decrease in chlorophyll and the increase in carotenoids and soluble solids content during fruit development is characteristic of papaya fruit development. The data corroborate the findings of Chan et al. (6). The relationship between subjective judgements of degrees of maturity and chemical determination of specific constituents forms the basis for our optical method of estimating papaya maturity.

The phenomenon involved in this work is transmittance of optical radiation through material having low or moderate absorption. Since the word "transmittance" has certain geometric connotations, the justification for using transmittance is that Beer's law is applicable on the microscopic scale. On the macroscale, the effective pathlength of the radiation through the tissue is dependent on the microscopic geometry, which results in light scattering. The phenomenon by which the color of a material is perceived visually is transmittance coupled with light scattering and the term "body reflectance" (2) was coined to describe the phenomenon in more familar terms. Body reflectance will be further defined as that radiation which leaves the material in the same area that is illuminated. Radiation leaving a material elsewhere will be termed "body transmittance". "Direct transmittance" is a special case of body transmittance which occurs when the sensitive surface of the detector is directly opposite the incident light source. This is the geometry normally used in spectrophotometry. Absorbance and other derivatives of absorption are reserved for those situations where the primary mechanism of attenuating the radiation is absorption. An optical density (OD) scale which refers to the log of the ratios of 2 transmittance measurements is used in this paper; i.e., a standard T_s and a specimen T, so OD = log (T_s/T), where there is no implication of how the radiation is attenuated. A translucent Vitrolite tile was used as a standard. The standard has low absorption and provides a means of eliminating the wavelength-dependent characteristics of the instrument in the data processing.

Table 1. Carotenoid, chlorophyll, and soluble solids contents for the different stages of maturity of papaya fruit.

Maturity category	No. fruit	Carotenoids (μg/g fresh wt)	Chlorophyll (μg/g fresh wt)	Soluble solids (%)
Immature	8	24.1 a[z]	37.3 a	5.6 a
Mature green	8	30.8 b	21.5 b	11.9 b
¼ ripe	8	41.3 c	10.2 cd	14.3 cd
½ ripe	8	45.0 d	4.0 d	13.4 d
Full ripe	8	51.1 d	2.3 d	15.1 d

[z]Mean separation based on overlapping 95% confidence limits using 2nd-degree polynominal analysis.

Since the pigment changes associated with the change from immature to mature-green fruit take place in the flesh and not in the skin, a body transmittance measurement was required. A critical part of this research approach centers around the capability of varying the sample-detector geometry (the physical arrangement). Three different sample-detector geometries were used in this work to make measurements of direct transmittance, body reflectance, and body transmittance.

We attempted to use the direct transmittance geometry used for detection of hollow-heart in potatoes (4), but the transmitted radiation was insufficient to produce a useful signal from the PMT. The optically dense green papaya and the thick mass of dark seeds in the center cavity of the more mature fruit made it difficult to get reliable data in a direct transmittance geometry. Additionally, we found that body reflectance spectra of intact papayas, measured with the sample-detector geometry shown in Fig. 1, could be used to separate the stages of maturity from color break to ripe, but reflectance measurements were not satisfactory for separating immature and mature-green fruit.

To develop a measurement to indicate pigmentation changes in the flesh of papaya, it is helpful to know how the radiation is redistributed in the fruit tissue. The physical basis for making these spectral measurements and the potential for using the proposed geometry is illustrated in Fig. 3 which shows that in the papaya radiation spreads out in all directions from the point of incidence. This observation was described in an earlier paper (2), and is the basis for a system designed to measure radiation that exists from the fruit close to the area illuminated (Fig. 2).

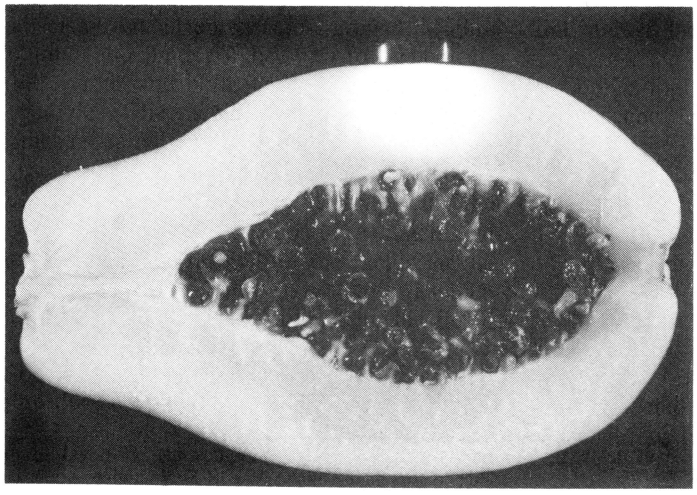

Fig. 3. Longitudinal section of mature-green papaya illustrating the internal distribution of radiation. Fruit is lighted on the top surface with a microscope illuminator.

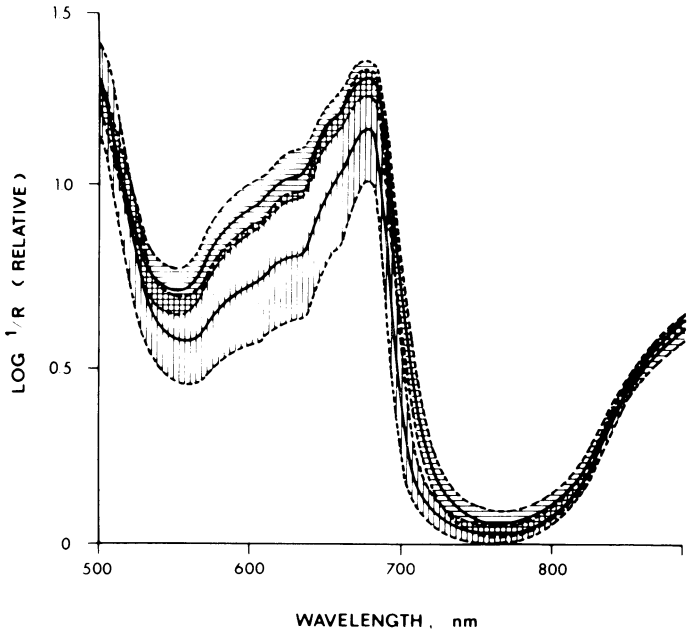

Fig. 4. Reflectance (Log $\frac{1}{R}$) curves of immature (horizontal crosshatching) and mature-green papaya (vertical crosshatching). The solid lines are the means of measurements on 5 fruit. The envelope is defined by ± 1 SD from the mean. These data were obtained with the sample geometry shown in Fig. 1.

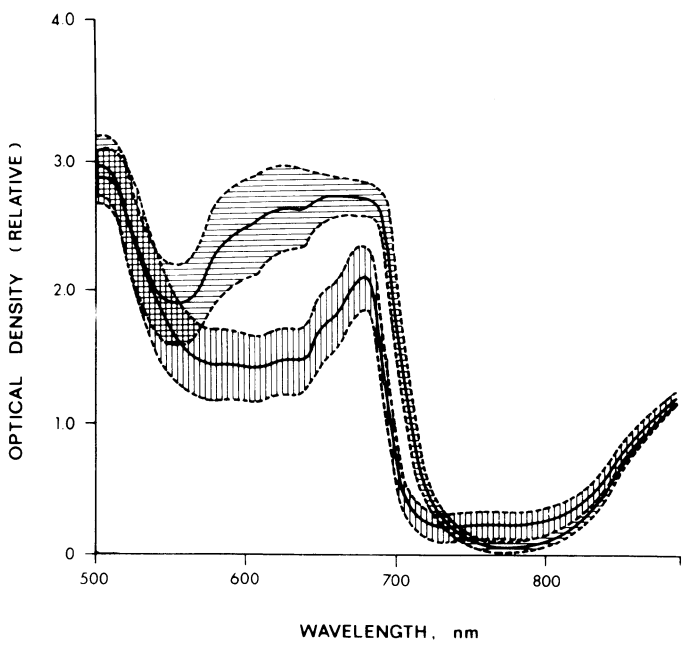

Fig. 5. Body transmittance (Log $\frac{1}{T}$) curves of immature (horizontal crosshatching) and mature-green papaya (vertical crosshatching). The solid lines are means of measurements of 5 fruit. The envelope is defined by ± 1 SD from the mean. These data were obtained with the sample geometry shown in Fig. 2.

This provides a workable system for determining pigment concentration in the fruit flesh as a means of separating immature from the mature-green papaya fruit.

We compared body reflectance and body transmittance measurements in our efforts to distinguish between immature and mature-green fruit. The results obtained with body reflectance measurements (Fig. 4) show that the mean curves (for 5 fruit) are different for the 2 maturity classes (immature and mature-green), but there is so much overlap of the envelope defined by the ± 1 standard deviation (SD) that it is doubtful a useful separation of these maturity classes could be achieved.

The body transmittance measurements (Fig. 5) showed considerable separation of the 2 envelopes. The slopes of the curves in the wavelength regions of 550–600 nm, 650–670 nm, and 710–740 nm are different for the 2 classes. Measurements obtained in the 650–690 nm region should be interpreted with caution; the curve shape in this spectral region should be the typical Gaussian curve shape of an absorption band. The flattened curve shape for the immature fruit in this region is due to stray light from the monochromator and possible fluorescence from the fruit (9). If these sources of error were not present, the shape of the curve for the immature fruit would be similar to that of the mature fruit, and the immature fruit would have still higher optical density values in the 650–690 nm range.

The correlation between pigment concentrations and soluble solids was determined in 2 different experiments. Expt. 1 involved the biological spectrophotometer using 25 fruit selected from 5 maturity categories. The constants and wavelengths required to predict the pigment concentrations with equation 1 along with correlation coefficients are given in Table 2. Our interpreation is that the primary indicator of maturity is chlorophyll concentration. The correlations between optical data and concentration of carotenoids and soluble solids are indications of the relationship between these parameters and the maturity of the fruit as predicted from changes in chlorophyll concentrations; however, these should not be interpreted as direct measures of carotenoid and soluble solids.

Body transmittance geometry (Fig. 2) measurements in expt. 2 were made on 40 fruit from 5 maturity categories using the tilting-filter instrument. Interference filters with nominal wavelengths of 590 nm, 680 nm, and 740 nm were installed. Correlations between optical and chemical data at the 1% level are listed in Table 2. There were no significant differences in correlations for any one constituent in the 2 experiments, as determined using the procedures outlined by Morrison (10). Therefore, the tilting filter can be used with papaya fruit to make the same maturity-predicting measurements as the biological spectrophotometer.

The tilting-filter instrument was used in a 3rd experiment designed to test the system's ability to distinguish between immature and mature-green fruit. Twenty papaya fruit, whose degree of ripeness was indistinguishable by appearance, were selected from a lot of presumably immature and mature-green fruit for optical measurements using body transmittance geometry. After

Table 2. Equation constants and correlation coefficients for predicting the concentrations of chlorophyll, carotenoids, and soluble solids in papaya.

	Expt. 1[z]						Expt. 2[y]
Constituent	K_0	K_1	λ_1 (nm)	K_2	λ_2 (nm)	r	r
Chlorophyll	4.34	330	620	−120	588	0.94	0.97
Carotenoids	30.8	−315	643	−317	520	0.92	0.94
Soluble solids	3.76	39.6	714	− 24.3	582	0.93	0.90

[z]Results obtained with biological spectrophotometer, N = 25 fruit.
[y]Results obtained with tilting-filter instrument, N = 40 fruit.

the optical data were recorded, the fruit were held 7 days at 20°C and then were cut open to determine the degree of ripening. Nine mature-green fruit had ripened or begun to ripen out of 20 fruit, while 10 immature fruit remained totally green. One fruit developed a soft rot and was not evaluated.

The derivative data at each wavelength were compared with the maturity rating by analysis of variance. A value of -1 was assigned to each of the 10 immature fruit and a $+1$ to each of the 9 fruit which ripened. The F statistic, which must exceed 8.40 for a 99% confidence level, was used as an indicator of performance in separating the 2 maturity categories. The wavelength regions where F exceeded 160 are shown in Fig. 6. The maximum F value in this experiment was 829 and was obtained with derivative data at 665 nm.

The wavelength regions given in Fig. 6, which were used in separating immature and mature-green papayas with the tilting-filter instrument, corresponded closely to the optimum wavelength regions indicated for this separation with the biological spectrophotometer, as discussed for Fig. 5. Therefore, the tilting-filter spectrophotometer, used in conjunction with the body-transmittance geometry, can make the spectral measurements on papayas required to separate them into maturity categories ranging from immature to ripe.

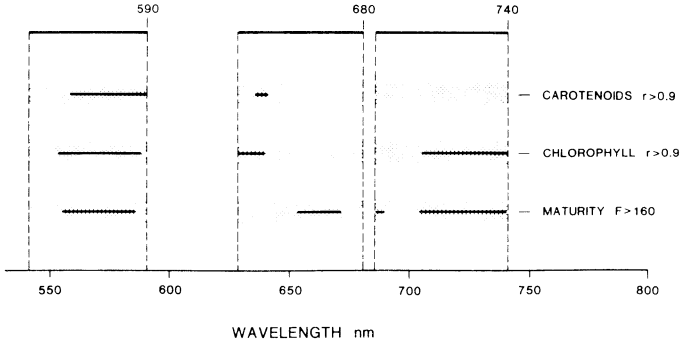

Fig. 6. Results obtained with the tilting-filter instrument. The horizontal lines at the top indicate the wavelength range covered by the filters. The horizontal lines corresponding with the pigments defined on the right indicate wavelength regions where high correlations (above 0.9) were obtained between the optical data and pigment concentration. The horizontal lines corresponding to maturity indicate wavelengths where the F value exceeded 160 for separating immature from mature-green fruit of papaya. The maturity separation was based on 2 classifications of a visual color score following a one-week storage period at 20°C after the optical data were recorded.

Literature Cited

1. Akamine, E.K. and T. Goo. 1971. Relationship between surface color development and total soluble solids in papaya. HortScience 6:567–568.
2. Birth, G.S. 1978. The light scattering properties of foods. J. Food Sci. 43:916–925.
3. Birth, G.S. 1979. Radiometric measurement of food quality—a review. J. Food Sci. 44:949–953.
4. Birth, G.S. and K.H. Norris. 1965. The difference meter for measuring interior quality of foods and pigments in biological tissues. U.S. Dept. Agr. Bul. 1341.
5. Birth, G.S. and G.L. Zachariah. 1973. Spectrophotometer for biological applications. Trans. Amer. Soc. Agr. Eng. 16:371–372.
6. Chan, H.T., Jr., K.L. Hibbard, T. Goo, and E.K. Akamine. 1979. Sugar composition of papayas during fruit development. HortScience 14:140–141.
7. Chen, N.K.L. 1964. Some chemical changes occurring during the postharvest ripening of papaya fruit. Bot. Bul. Acad. Sinic. 1:89–99.
8. Harborne, J.B. 1973. Phytochemical methods. Chapman and Hall, London.
9. Massie, D.R. and K.H. Norris. 1976. A high intensity spectrophotometer interfaced with a computer for food quality measurement, p. 12–15. In: J.J. Gaffney (ed.). Quality detection in foods. Amer. Soc. Agr. Eng. Pub. 1–76. St. Joseph, Mich.
10. Morrison, D.F. 1976. Multivariate statistical methods. 2nd ed. McGraw-Hill, New York.
11. Rosenthal, R.D. 1978. An introduction to near infrared quantitative analysis. Neotec Instruments, 2431 Linden Lane, Silver Spring, MD 20910.
12. Seo, S.T., G.J. Farias, and E.J. Harris. 1982. Oriental fruit fly: ripening of fruit and its effect on the index of infestation of Hawaiian papayas. J. Econ. Entomol. 75:173–178.